



Contents lists available at ScienceDirect



# Catalysis Today

journal homepage: [www.elsevier.com/locate/cattod](http://www.elsevier.com/locate/cattod)

## An efficient and sustainable production of triacetin from the acetylation of glycerol using magnetic solid acid catalysts under mild conditions

Jinyan Sun, Xinli Tong\*, Linhao Yu, Jun Wan\*

Tianjin Key Laboratory of Organic Solar Cells and Photochemical Conversion, School of Chemistry and Chemical Engineering, Tianjin University of Technology, Tianjin 300384, P. R. China

### ARTICLE INFO

#### Article history:

Received 4 May 2015

Received in revised form 4 July 2015

Accepted 11 July 2015

Available online xxx

#### Keywords:

Glycerol

Acetylation

Triacetin

Magnetic material

Solid acids

### ABSTRACT

The efficient and selective acetylation of glycerol to produce triacetin is achieved using magnetic solid acids as catalysts. The Fe-based materials including  $\text{Fe-Sn-Ti(OH)}_x$ ,  $\text{Fe-Sn-Ti(SO}_4^{2-}\text{)}$  and  $\text{Fe-Sn-Ti(SO}_4^{2-}\text{-}t$  ( $t$  represents the temperature for the heating treatment) were successfully prepared and employed in the acetylation of glycerol, respectively. As a result, 100% conversion and 99.0% selectivity for triacetin was obtained in the presence of a catalytic amount of  $\text{Fe-Sn-Ti(SO}_4^{2-}\text{-}400$  at  $80^\circ\text{C}$  for 30 min, which exhibits higher catalytic activity than those of some molecular sieves. The magnetic catalytic materials were respectively characterized by XRD, IR, TG-DTG, BET and  $\text{NH}_3$ -TPD techniques. Moreover, the effects of reaction temperature and reaction time in the glycerol acetylation are investigated in detail. Finally, based on the experimental results and reaction phenomena, a possible mechanism for the catalytic reaction is proposed.

© 2015 Elsevier B.V. All rights reserved.

### 1. Introduction

The rapid increase of biodiesel production has led to a wider availability of crude glycerol as a by-product in chemical industry. Thus, the efficient utilization of excessive and cheap glycerol are becoming a new research topic at present, in which the etherification [1,2] and esterification processes [3,4] to fuel additive are considered as the promising route to conversion of glycerol.

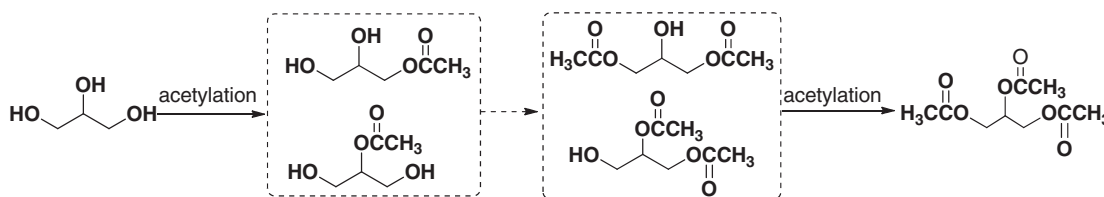
The glycerol derivatives such as glycerol esters, acetyl glycerol and glycerol acetal have good potential for the usage as fuel components that assist to a decreasing in particles, hydrocarbons, carbon monoxide and unregulated aldehydes emission. As shown in Scheme 1, the acetylation of glycerol contains three main steps, involving consecutive formations of monoacetin, diacetin, and triacetin via esterification reaction in the presence of acetylation reagents. In the previous study, the glycerol acetylation process was often accelerated by the acid catalysts in homogeneous media, for example, over sulfuric acid, hydrofluoric acid, *p*-toluenesulfonic acid or acidic ionic liquids [5,6]. However, these mineral acid catalysts have the obvious disadvantages such as the severe

environmental and economic issues. For avoiding these problems, the acetylation of glycerol with acetic acid was extensively studied in the presence of solid catalysts [3,7,8]. Generally, the used heterogeneous catalysts included the acid exchange resins [9–11], K-10 montmorillonite, HZSM-5 [3], HUSY [8], niobium-zirconium mixed oxides [12], PMo-NaUSY [13], supported heteropolyacids [14–16], mesoporous silica [17], and sulfonic acid functionalized deoxycellulose [18], sulfated zirconia and niobic acid [19] etc. Particularly, the cation-exchange resins showed the high catalytic activity as well as the selectivity of higher esters where the triacetin are lower compared to diacetin. Very recently, Huang et al. [20] reported that the acetylation of glycerol to triacetin was achieved with the heteropolyacid-based ionic liquids as catalysts in which a 100% conversion of glycerol and a superior selectivity (86–99%) was obtained. Khayoon et al. [21] found that the Y/SBA-3 catalyst could promote the formation of diacetin and triacetin in the glycerol acetylation where the selectivity of 34% and 55% toward diacetin and triacetin was achieved under suitable conditions. Kale et al. [22] investigated the esterification of glycerol with acetic acid over acidic Amberlyst ion-exchange resins in the presence of toluene as an entrainer. As a result, a 95% selectivity of triacetin at complete glycerol conversion was obtained.

In this study, a series of magnetic solid catalysts and molecular sieves were successfully prepared and further employed in the acetylation of glycerol under mild conditions. It is found that a 100%

\* Corresponding authors. Tel./fax: +86 22 60214259.

E-mail addresses: [tongxlini@tju.edu.cn](mailto:tongxlini@tju.edu.cn), [tongxli@hotmail.com](mailto:tongxli@hotmail.com) (X. Tong), [wanjuntjljg@sina.com](mailto:wanjuntjljg@sina.com) (J. Wan).



conversion and 99.0% selectivity for triacetin was obtained using the Fe-Sn-Ti( $\text{SO}_4^{2-}$ )-400 as the catalyst at 80 °C for 30 min. Moreover, based on the reaction phenomena and experimental results, a possible reaction mechanism is proposed to explain the catalytic process.

## 2. Experimental

### 2.1. Reagents and instruments

Glycerol, ferrous sulfate, ferric sulfate, stannic chloride pentahydrate, acetic acid, ammonia, tin(II) acetate, NaOH, acetic anhydride, ammonium sulfate, HZSM-5, H- $\beta$  zelite, nitric acid, deionized water and ethanol are analytic grade and got from commercial sources.

The monoaceton, diacetin and triacetin as the standard samples are purchased from Alfa Aesar.

The measurement of X-ray diffraction (XRD) was performed by diffractometer with Cu K $\alpha$  radiation (0.02° resolution) and was collected from 20 to 80° [20]. The spectra of Fourier transform infrared spectroscopy (FT-IR) are recorded on a Nicolet Nexus spectrometer in the 400–4000 cm $^{-1}$  range. The thermal analysis (TG-DTG) is performed with NETASCH TG 209F3 instrument, and the data are shown from 0–1000 °C. BET surface areas, pore volumes, and average pore diameters of the prepared samples are obtained from N<sub>2</sub> (77 K) adsorption measurement using a Micromeritics ASAP2020 M system, in which the samples are pretreated under vacuum at 150 °C for 4 h before the measurement. The average pore diameters are calculated according to Barrett–Joyner–Halenda (BJH) model in absorption and desorption period. The acid properties of the magnetic solid catalysts was determined by temperature-programmed desorption of ammonia (NH<sub>3</sub>-TPD). Before the adsorption of ammonia the samples were treated under helium at 500 °C (from 25 to 500 °C in 40 min) for 1 h. The samples were then cooled to 25 °C in He flow, then treated with a NH<sub>3</sub> flow for 30 min at 100 °C. The physisorbed ammonia was eliminated by flowing He for 1 h at 100 °C. NH<sub>3</sub>-TPD was run between 100 °C and 950 °C at 10 °C/min and followed by an online gas chromatograph (GC) provided with a thermal conductivity detector.

The quantitative analyses of the products are performed on a GC apparatus with FID detector. The capillary column is HP-5, 30 m × 0.25 mm × 1.0  $\mu\text{m}$ . In addition, the qualitative analysis for the product is carried out on the Agilent 6890/5973 Gas Chromatograph-Mass Spectrometer (GC-MS) instrument.

### 2.2. The preparation of magnetic matrix and its treatment method

The typical procedure is given in the following: a mixture of ferrous sulfate/ferric sulfate [ $\text{Fe}_2\text{SO}_4/\text{Fe}_2(\text{SO}_4)_3$ ] was added in a vessel and solved with deionized water. The solution was then heated to 45 °C and NH<sub>3</sub>·H<sub>2</sub>O was added to adjust pH value to 10–11 using acidometer. The reaction was kept for 1 h. The produced magnetic matrix was separated with magnetic separation method and washed repeatedly to the neutrality. The magnetic matrix was stored with suspension liquid to use.

### 2.3. The synthesis of Fe-Sn-Ti ( $\text{SO}_4^{2-}$ ) solid acid

Stannic chloride pentahydrate (17.5 g) is added in three-neck flask. Under rapid stirring, 15 mL magnetic matrix (0.1 mol/L) and 10 mL tetrabutyl titanate are poured into the above flask, and then NH<sub>3</sub>·H<sub>2</sub>O is slowly dropped into the mixture to form the pasty liquids. The produced solid is filtered and washed numerous times to be neutral. Then, the solid sample is dried at 100 °C in oven, and the obtained material is referred as Fe-Sn-Ti (OH)<sub>x</sub>. In the following, the above solid product is further sulfated through being soaked with 1 mol/L (NH<sub>4</sub>)<sub>2</sub>SO<sub>4</sub> solution for 24 h, and then filtered, dried to obtain the sulfated Fe-Sn-Ti material that is referred as Fe-Sn-Ti ( $\text{SO}_4^{2-}$ ). In addition, the sulfated Fe-Sn-Ti materials are calcined at different temperatures. Therein, the obtained samples calcined at 400 °C, 500 °C, 600 °C and 700 °C are signified by the Fe-Sn-Ti ( $\text{SO}_4^{2-}$ )-400, Fe-Sn-Ti ( $\text{SO}_4^{2-}$ )-500, Fe-Sn-Ti ( $\text{SO}_4^{2-}$ )-600 and Fe-Sn-Ti ( $\text{SO}_4^{2-}$ )-700 in the next discussion.

### 2.4. The preparation of deAl- $\beta$ and Sn- $\beta$ zeolites

The preparation of the deAl- $\beta$  and Sn- $\beta$  zeolites is similar with the reference [23]. In brief, 1) deAl- $\beta$  zeolite is synthesized via the dealumination of H- $\beta$ . The commercial H- $\beta$  zeolite was dealuminated by treatment in HNO<sub>3</sub> solution (13 M) at 100 °C for 20 h [20 mL·g $^{-1}$ (zeolite)]. 2) The Sn- $\beta$  zeolite is synthesized by the solid-state ion-exchange (SSIE) process. The appropriate amount of tin(II) acetate was grinded with the required amount of dealuminated zeolite for 15 min. In addition, these prepared zeolites were calcined in an air flow at 550 °C before being used.

### 2.5. General procedure for the acetylation of glycerol

All the acetylations of glycerol with acetic anhydride or acetic acid were performed in a 120 mL steel autoclave equipped with the magnetic stirring and a temperature controller. Typical procedure for catalytic process is given as follows: a 1.5 g glycerol, 8.39 g acetic anhydride and the catalyst (2.5 wt.%) were charged into the autoclave; Under stirring, the mixture was preheated to 80 °C and kept for 30 min after the reactor was sealed. After the reaction, the mixture was transferred to a volumetric flask and was diluted with anhydrous ethanol. The conversion of glycerol and the selectivity of product were attained using the gas chromatograph with the internal standard method.

## 3. The physical properties of solid acid catalysts

### 3.1. The IR spectra of different catalysts

**Figure 1** shows the IR spectra of different catalytic materials including Fe-Sn-Ti(OH)<sub>x</sub>, Fe-Sn-Ti ( $\text{SO}_4^{2-}$ ), Fe-Sn-Ti ( $\text{SO}_4^{2-}$ )-400 and Fe-Sn-Ti ( $\text{SO}_4^{2-}$ )-600. It was found that the peaks of 3100–3250 cm $^{-1}$  and 3420–3550 cm $^{-1}$  in the spectrum of Fe-Sn-Ti(OH)<sub>x</sub> are attributed to the stretching vibration of combined water and O–H bond. Moreover, these peaks of water and O–H bond become weak after the Fe-Sn-Ti(OH)<sub>x</sub> is sulfated. Moreover, the characteristic peaks of the sulfated metal oxides often occur

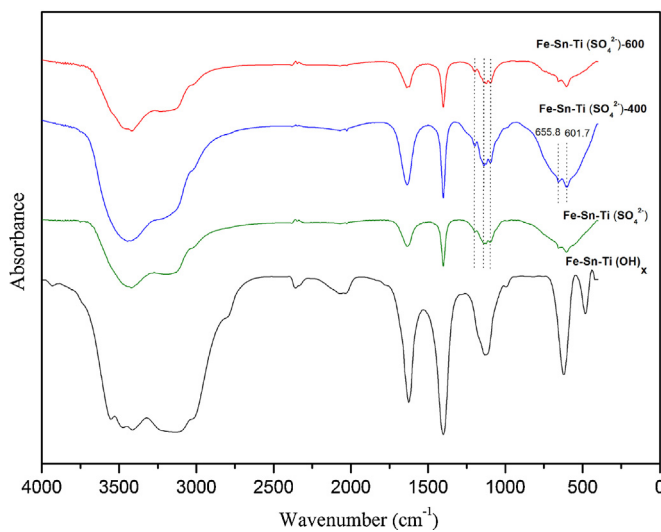


**Fig. 1.** The IR spectra of different magnetic catalytic materials.

between 900 and 1400 cm<sup>-1</sup>, assigned to the stretching vibrations of the S=O bond or S—O bond [24]. In the spectra of Fe-Sn-Ti (SO<sub>4</sub><sup>2-</sup>), Fe-Sn-Ti (SO<sub>4</sub><sup>2-</sup>)-400 and Fe-Sn-Ti (SO<sub>4</sub><sup>2-</sup>)-600, the typical new peaks of 1095.5 cm<sup>-1</sup>, 1141.8 cm<sup>-1</sup> and 1201.6 cm<sup>-1</sup> represent the formation of the superacid structures.

### 3.2. XRD patterns

In Fig. 2, the XRD patterns for the magnetic materials Fe-Sn-Ti (OH)<sub>x</sub>, Fe-Sn-Ti (SO<sub>4</sub><sup>2-</sup>), Fe-Sn-Ti (SO<sub>4</sub><sup>2-</sup>)-400, Fe-Sn-Ti (SO<sub>4</sub><sup>2-</sup>)-600 and Fe-Sn-Ti (SO<sub>4</sub><sup>2-</sup>)-700 are presented in which the crystal structures of these materials is indicated. The peaks at 26.749°, 34.061° and 52.228° are the characteristic diffraction of Titanium Tin Oxide [(Ti<sub>0.3</sub>Sn<sub>0.7</sub>)O<sub>2</sub>]. It indicates that there is the weak relationship of Ti-O-Sn bond in the Fe-Sn-Ti(OH)<sub>x</sub> and Fe-Sn-Ti (SO<sub>4</sub><sup>2-</sup>) materials. Furthermore, the new peaks at 38.100°, 54.935°, 58.355°, 62.258° and 65.185° begin to appear in the materials of Fe-Sn-Ti (SO<sub>4</sub><sup>2-</sup>)-400, Fe-Sn-Ti (SO<sub>4</sub><sup>2-</sup>)-500 and Fe-Sn-Ti (SO<sub>4</sub><sup>2-</sup>)-600 which are attributed to the formation of cassiterite. This shows that there exists a mutual function between Sn and Fe element for these catalytic materials. Otherwise, more peaks at 39.491° and 72.757° is shown up in the Fe-Sn-Ti (SO<sub>4</sub><sup>2-</sup>)-700 material. It is probably due to the stronger function appearing between Sn-O-Ti and Fe<sub>3</sub>O<sub>4</sub> support after high temperature treatment.

### 3.3. TG-DTG detection

The detection of TG-DTG of magnetic catalytic materials was performed and the results are shown in Fig. 3. It was found that there exists two obvious regions for the weight loss in the curve of Fe-Sn-Ti (OH)<sub>x</sub> material in which the scope of temperature is 40–100 °C and 130–600 °C domain. The first loss of weight is attributed to the remove of water absorbed in the surfaces of the material. The second weight loss should be due to the dehydration of Sn(OH)<sub>x</sub> and Ti(OH)<sub>4</sub> to form the oxides. In the TG-DTG graph of Fe-Sn-Ti (SO<sub>4</sub><sup>2-</sup>), the loss of weight appear in the region of 50–140 °C, 160–305 °C, 315–385 °C, 400–490 °C and 520–670 °C, respectively. The first and second loss of weight is contributed to the remove of water absorbed and hydroxide groups in the surfaces of the catalysts. The next other three losses of weight are contributed to the remove of SO<sub>x</sub> and the breakdown of acid structure. Besides, the TG-DTG detection of Fe-Sn-Ti (SO<sub>4</sub><sup>2-</sup>)-400 and Fe-Sn-Ti (SO<sub>4</sub><sup>2-</sup>)-600 materials was also performed, and the loss of weight appears in the region of 410–580 °C and 590–820 °C in the

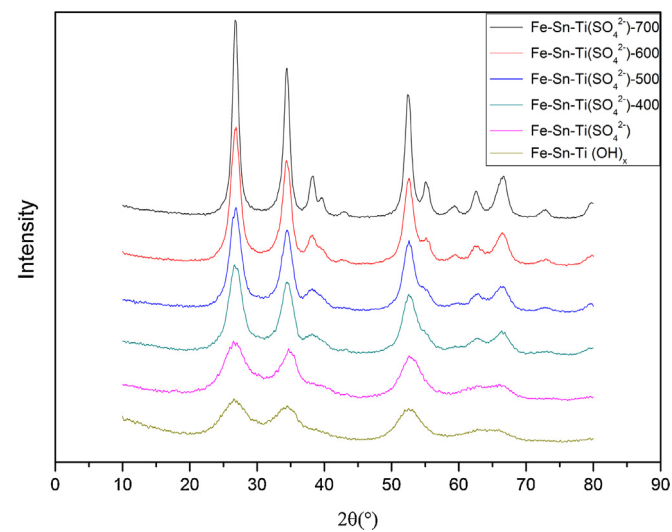


**Fig. 2.** The XRD patterns of different magnetic catalytic materials.

graph of Fe-Sn-Ti (SO<sub>4</sub><sup>2-</sup>)-400, while the loss of weight appears in the region of 620–830 °C in the graph of Fe-Sn-Ti (SO<sub>4</sub><sup>2-</sup>)-600 material. These indicates that the chelation of SO<sub>4</sub><sup>2-</sup> and metal–O bond has different states. The structure of superacid was partially destroyed after being calcined at 600 °C. The acid sites of Fe-Sn-Ti (SO<sub>4</sub><sup>2-</sup>)-600 is more confined than Fe-Sn-Ti (SO<sub>4</sub><sup>2-</sup>)-400 material.

### 3.4. BET measurement

Textural properties of the catalyst materials derived from the nitrogen physisorption are shown in Table 1. The results indicate that the surface area of solid catalyst is increased from 16.96 m<sup>2</sup> g<sup>-1</sup> to 18.88 m<sup>2</sup> g<sup>-1</sup> and the pore volume is also elevated to from 0.13 cm<sup>3</sup> g<sup>-1</sup> to 0.15 cm<sup>3</sup> g<sup>-1</sup> after being calcined at 400 °C. Then, the surface area is decreased along with the increase of the calcined temperature and the surface area is only 11.64 m<sup>2</sup> g<sup>-1</sup> for Fe-Sn-Ti (SO<sub>4</sub><sup>2-</sup>)-700 catalyst. Moreover, there is a certain increase in the average pore diameters with the elevation of the calcination temperature, in which the value of 2.8240 nm for Fe-Sn-Ti (SO<sub>4</sub><sup>2-</sup>) is increased to the value of 8.0875 nm for Fe-Sn-Ti (SO<sub>4</sub><sup>2-</sup>)-700 material.

### 3.5. NH<sub>3</sub>-TPD detection

In order to study acidic properties of magnetic solid catalysts, the NH<sub>3</sub>-TPD was performed from 100 to 950 °C, and the experimental results are presented in the Fig. 4. It can be seen that three peaks (212 °C, 529 °C and 718 °C) occur on the NH<sub>3</sub>-TPD profile of the Fe-Sn-Ti (SO<sub>4</sub><sup>2-</sup>)-400 catalyst. Herein, the first peak showed the existence of weak acidic sites, and the second peak indicated the co-existence of medium and strong acidic sites [25,26]. The third peak should be contributed to the self-decomposition of the catalyst. Similarly, there exist three kinds of peaks on the profile of the Fe-Sn-Ti (SO<sub>4</sub><sup>2-</sup>)-500 catalyst, while the amount of acidic sites (corresponds to peak area) is less than that of the Fe-Sn-Ti (SO<sub>4</sub><sup>2-</sup>)-400 catalyst. In case of the Fe-Sn-Ti (SO<sub>4</sub><sup>2-</sup>)-600 catalyst, the amount of acidic sites become much less than the above two catalysts. Especially, the weak acid nearly disappeared. Furthermore, no apparent peak come out on the NH<sub>3</sub>-TPD profile of the Fe-Sn-Ti (SO<sub>4</sub><sup>2-</sup>)-700 catalyst, which showed that no acidic sites were generated on this catalyst.

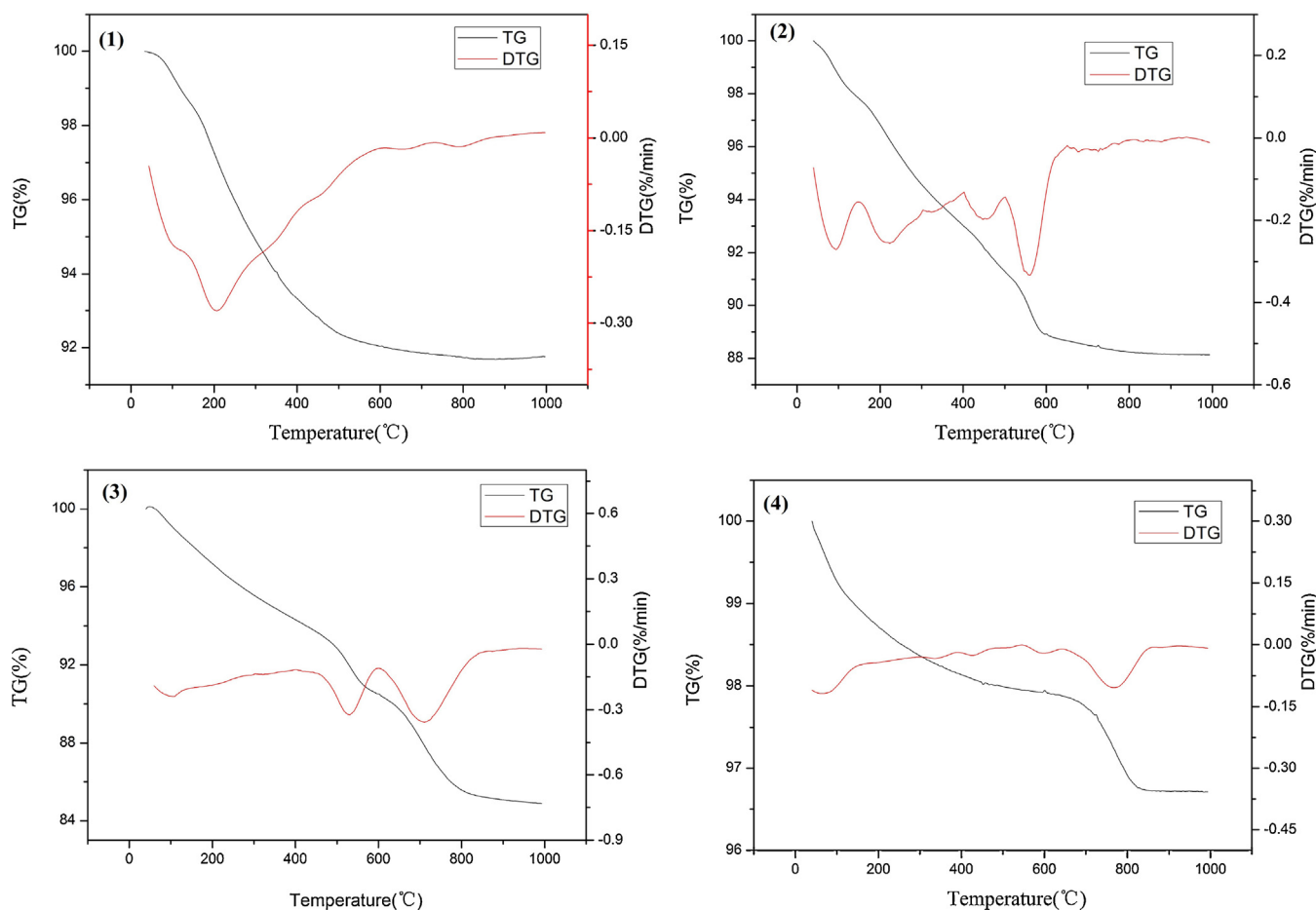


**Fig. 3.** The TG-DTG result for different magnetic catalytic materials [(1) refers to Fe-Sn-Ti ( $\text{OH}_x$ ); (2) refers to Fe-Sn-Ti ( $\text{SO}_4^{2-}$ ); (3) refers to Fe-Sn-Ti ( $\text{SO}_4^{2-}$ )-400; (4) refers to Fe-Sn-Ti ( $\text{SO}_4^{2-}$ )-600].

## 4. Results and discussion

### 4.1. The acetylation of glycerol to triacetin by the magnetic catalytic material

In the beginning, the catalytic performance of different solid acids is first investigated in the acetylation of glycerol with acetic anhydride (shown in Scheme 2), in which a series of magnetic materials, zeolites and Amberlyst-15 was employed as the catalysts. As comparison, the blank experiment was also performed. The obtained experimental results are summarized in Table 2.

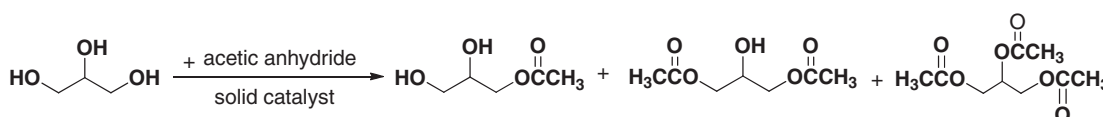
Seen from the experimental data, it is found that 49% conversion of glycerol was obtained in the absence of any catalyst where the selectivity of monoacetin, diacetin and triacetin is 48%, 46% and 6%, respectively (entry 1). With the Fe-Sn-Ti ( $\text{SO}_4^{2-}$ ) as the catalyst, a 58% conversion and 83% selectivity of monoacetin is attained

(entry 2). To our surprise, the conversion is increased to 100% and selectivity of triacetin reaches 99% when the Fe-Sn-Ti( $\text{SO}_4^{2-}$ )-400 was employed as the catalyst (entry 3). Moreover, a 99% conversion of glycerol in 97% or 96% selectivity of triacetin was obtained in the presence of Fe-Sn-Ti ( $\text{SO}_4^{2-}$ )-500 or Fe-Sn-Ti ( $\text{SO}_4^{2-}$ )-600 catalyst (entries 4 and 5). This should be due to the promotion of the formed structure of superacid in the reaction. In addition, based on the results of  $\text{NH}_3$ -TPD measurements, the amount of acid on the Fe-Sn-Ti ( $\text{SO}_4^{2-}$ )-600 catalyst is much less than that on the Fe-Sn-Ti ( $\text{SO}_4^{2-}$ )-400 catalyst; besides, there very little weak acidic sites exist on the Fe-Sn-Ti ( $\text{SO}_4^{2-}$ )-600 catalyst. Thus, it can be concluded that the catalytic activity is closely related to the acid strength of catalyst and the amount of acid is not a determining factor. However, the conversion of glycerol is reduced to 68% and monoacetin become main product as much as 82% selectivity in the presence of Fe-Sn-Ti ( $\text{SO}_4^{2-}$ )-700 catalyst (entry 6). It is comparable to the

**Table 1**  
the BET data for different acid catalysts.

Catalysts	BET surface area ( $\text{m}^2 \text{g}^{-1}$ )	Pore volume ( $\text{cm}^3 \text{g}^{-1}$ )		Average pore diameter (nm)	
		BHJ adsorption	BHJ desorption	BHJ adsorption	BHJ desorption
Fe-Sn-Ti( $\text{SO}_4^{2-}$ )	16.9606	0.127524	0.128372	2.8240	2.9477
Fe-Sn-Ti( $\text{SO}_4^{2-}$ )-400	18.8818	0.145857	0.153853	4.2046	3.7972
Fe-Sn-Ti( $\text{SO}_4^{2-}$ )-500	16.5536	0.134225	0.141268	5.2298	4.6957
Fe-Sn-Ti( $\text{SO}_4^{2-}$ )-600	14.9134	0.123552	0.134966	6.1426	5.6663
Fe-Sn-Ti( $\text{SO}_4^{2-}$ )-700	11.6472	0.077765	0.110199	8.0875	9.2812

Volume of pores cumulated between 17.000 Å and 3,000.000 Å diameter.

**Scheme 2.** The catalytic acetylation of glycerol with acetic anhydride in the presence of acid catalyst.**Table 2**The acetylation of glycerol and acetic anhydride with different catalysts<sup>a</sup>

Entry	Catalyst	Conv. (%) <sup>b</sup>	Product distribution (%) <sup>b</sup>		
			Monoacetin	Diacetin	Triacetin
1	Blank	49	48	46	6
2	Fe-Sn-Ti ( $\text{SO}_4^{2-}$ )	58	83	17	0
3	Fe-Sn-Ti ( $\text{SO}_4^{2-}$ )-400	100	0	1	99
4	Fe-Sn-Ti ( $\text{SO}_4^{2-}$ )-500	99	0	3	97
5	Fe-Sn-Ti ( $\text{SO}_4^{2-}$ )-600	99	0	4	96
6	Fe-Sn-Ti ( $\text{SO}_4^{2-}$ )-700	68	82	17	1
7	Sn- $\beta$	89	59	37	4
8	deAl- $\beta$	74	78	21	1
9	HZSM-5	99	14	62	24
10	Amberlyst-15	99	0	1	99
11 <sup>c</sup>	Fe-Sn-Ti ( $\text{SO}_4^{2-}$ )-400	99	13	61	26

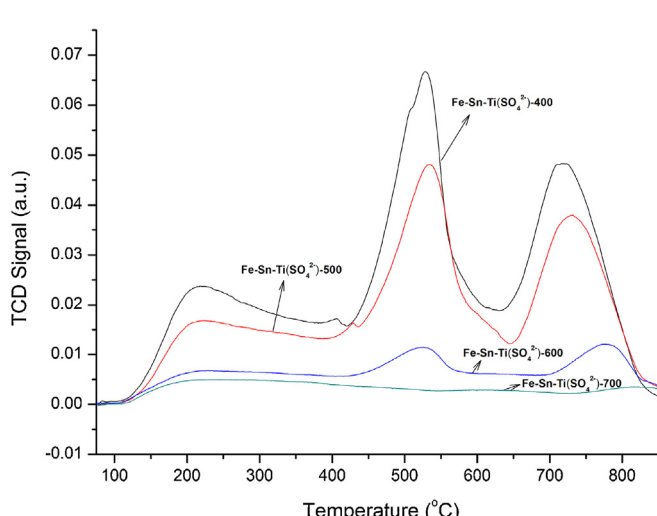
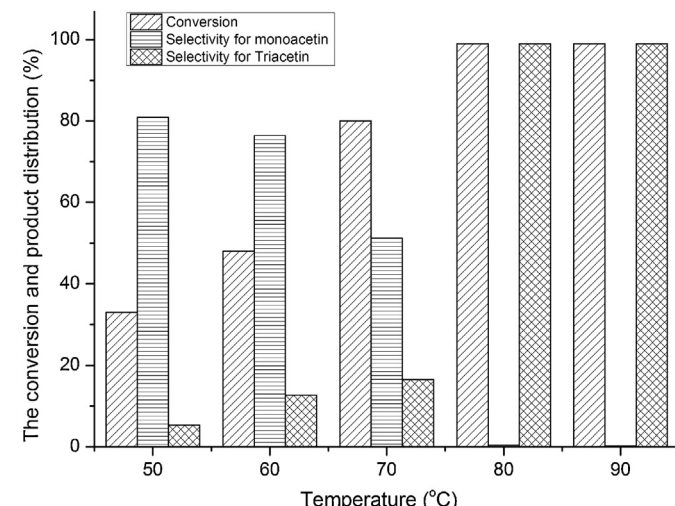
<sup>a</sup> Reaction conditions: glycerol 1.5 g, acetic anhydride 8.39 g and 0.05 g catalyst is added, at 80 °C, for 30 min under magnetic stirring.<sup>b</sup> The data are obtained by GC with the internal standard method.<sup>c</sup> About 1 mL H<sub>2</sub>O is added into reaction mixture.

result of acetylation reaction using uncalcined Fe-Sn-Ti ( $\text{SO}_4^{2-}$ ) catalyst which matches the disappear of superacid after being treated at 700 °C high temperature. Furthermore, some common acid catalysts were also studied in the acetylation of glycerol under similar conditions. As a result, it was found that 89% or 74% conversions was obtained using the molecular sieve Sn- $\beta$  or deAl- $\beta$  as the catalyst, respectively; meanwhile, the major products are monoacetin and diacetin (entries 7 and 8). In the presence of HZSM-5 catalyst, the conversion of glycerol arrived at 99%, and the selectivity of diacetin and triacetin was respectively 62% and 24% (entry 9), which can be attributed to the occurrence of the stronger acidic sites. Also, the Amberlyst-15 is employed as the solid catalyst and a 99% conversion in 99% selectivity of triacetin was attained (entry 10). This is near to the data with magnetic solid catalytic materials. On the other hand, with the Fe-Sn-Ti ( $\text{SO}_4^{2-}$ )-400 catalyst, the selectivity of triacetin is decreased to 26% and the selectivity of monoacetin and diacetin is elevated to 13% and 61% when 1 mL

pure H<sub>2</sub>O is added into reaction mixture; meanwhile, the conversion of glycerol was still 99% (entry 11). It exhibits that more water is disadvantageous to the production of triacetin in this catalytic process.

#### 4.2. The effect of temperature on the acetylation of glycerol

In the following, the influence of temperature on the acetylation of glycerol with acetic anhydride in the presence of the Fe-Sn-Ti ( $\text{SO}_4^{2-}$ )-400 catalyst was investigated and the results are shown in Fig. 5. It can be seen that the conversion of glycerol is gradually elevated, and the selectivity of monoacetin decreases and the selectivity of triacetin slowly increases along with the temperature being increased from 50 °C to 80 °C. Furthermore, the conversion and the product distribution is almost unchanged when the temperature was increased to 90 °C in the reaction.

**Fig. 4.** The NH<sub>3</sub>-TPD profiles of different magnetic solid catalysts.**Fig. 5.** Effect of temperature in the acetylation of glycerol with Fe-Sn-Ti ( $\text{SO}_4^{2-}$ )-400 catalyst.

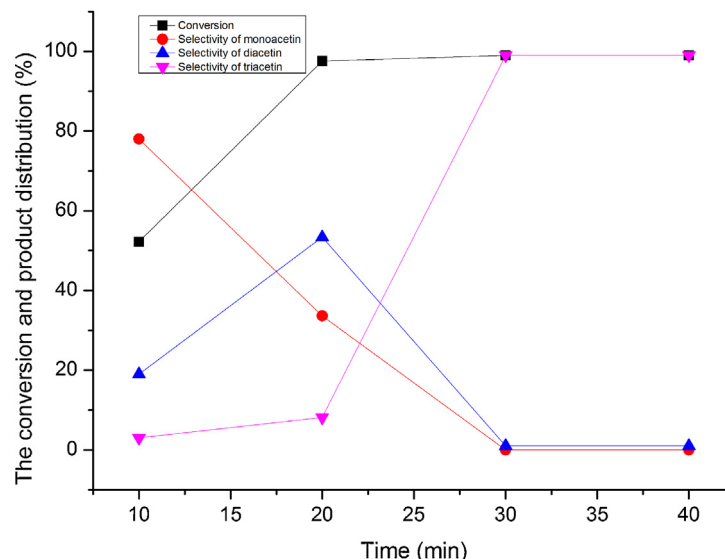


**Fig. 6.** Effect of time in the acetylation of glycerol with Fe-Sn-Ti( $\text{SO}_4^{2-}$ )-400 catalyst.

#### 4.3. Effect of reaction time on the acetylation of glycerol

**Fig. 6** showed the effect of reaction time on the acetylation of glycerol with acetic anhydride in the presence of the Fe-Sn-Ti( $\text{SO}_4^{2-}$ )-400 catalyst. As a result, it was found that the conversion of glycerol gradually increases along with the reaction time being increased from 10 min to 30 min, in which the selectivity of monoaceton is slowly decreased, and the diacetin selectivity was firstly increased to top value and then decreased, and the selectivity of triacetin was increased all the time. These characters are completely suitable for the typical consecutive reaction. Moreover, the conversion of glycerol and product selectivity almost keep unchanged after being further reacted for 40 min and more period.

#### 4.4. The acetylation of glycerol with acetic acid under different temperatures

In order to further reveal the character of acetylation of glycerol using magnetic catalytic materials, the acetic acid is employed as the acetylating reagent at different temperatures. The experimental results are presented in **Fig. 7**. As a result, the main product is monoaceton and the by-product is diacetin when acetic acid replaced the acetic anhydride in the reaction. Therein, a 32.3% conversion and 100% selectivity of monoaceton was obtained when the reaction was performed at 80 °C. Along with the elevation of temperature, the conversion was gradually increased and the selectivity was slowly reduced. When the temperature is increased to 140 °C, the conversion and selectivity of monoaceton is respectively 75.7% and 90.3%.

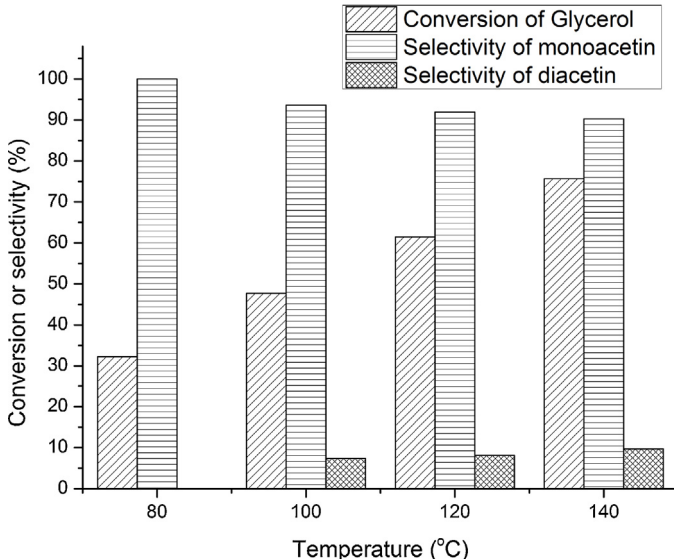


**Fig. 7.** The acetylation of glycerol with acetic acid by Fe-Sn-Ti( $\text{SO}_4^{2-}$ )-400 catalyst (Reaction conditions: 1.5 g glycerol, acetic acid 9.79 g and 0.05 g catalyst is employed, for 30 min, under the magnetic stirring).

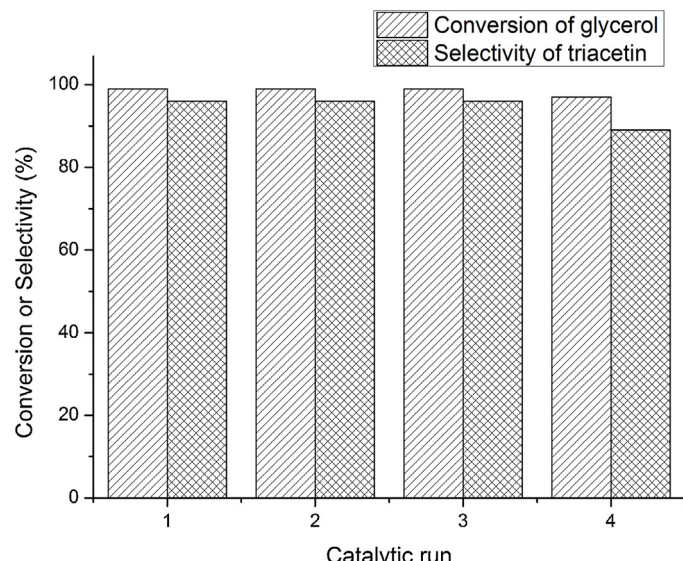


**Fig. 8.** The recycling of the Fe-Ti-Sn( $\text{SO}_4^{2-}$ )-400 catalyst in the acetylation of glycerol.

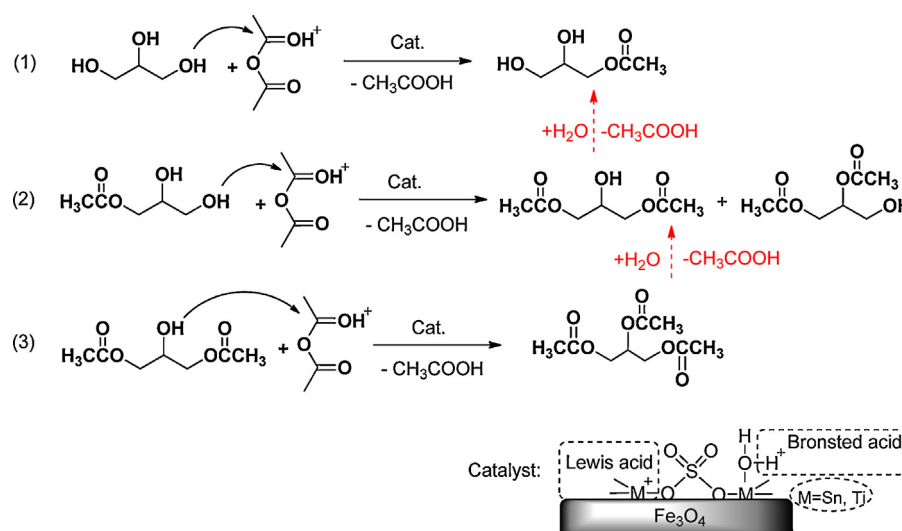


**Fig. 9.** Reaction mechanism on the acetylation of glycerol with magnetic catalyst.

#### 4.5. The investigation on the recycling of catalyst

The recycling of the magnetic catalyst has been examined. It should be mentioned that the catalysts is easily separated from the reaction mixture owing to its own magnetic performance. The investigations are performed at 80 °C for 30 min in the presence of Fe-Ti-Sn (SO<sub>4</sub><sup>2-</sup>)-400 catalyst. After the reaction, the solid catalyst is separated from the reaction solution with the assistance of the magnet. It is first washed with ethanol for 3 times, and then is dried and calcined at 400 °C for 3 h in the oven. The obtained magnetic catalyst is further used in the next run by adding the glycerol and acetic anhydride as reactants. In Fig. 8, it can be seen that the yield of triacetin almost keeps unchanged in the former three recycled reactions which shows that the catalyst retains a very high activity for the acetylation of glycerol. Furthermore, the yield of triacetin decreases a little (about 9%) after being recycled four times. All these results indicate that the magnetic catalytic material is efficient and recycled in the glycerol acetylation.

#### 4.6. The reaction mechanism for the acetylation of glycerol

Based on the obtained results and reaction phenomena, a possible catalytic reaction mechanism has been proposed (see Fig. 9). First, acetic anhydride can function with solid acid catalyst in which carbonyl group is activated with hydrogen proton or Lewis acid site. Then, the activated carbonyl of acetic anhydride is attacked by the glycerol molecule to generate the monoacetyl along with the lose of a acetic acid molecule. Furthermore, the monoacetyl reacts with activated carbonyl group of another molecular acetic anhydride, which leads to produce the diacetin (e.g. 2-hydroxypropane-1,3-diyl diacetate and 3-hydroxypropane-1,2-diyl diacetate). Finally, the activated carbonyl group of third acetic anhydride is further attacked by the diacetin, and the triacetin is obtained with the lose of a molecular acetic acid. According the principle of reversible reaction, the diacetin and triacetin can probably be converted to monoacetyl and diacetin during the whole process if there exists a certain water molecule (shown in dotted line). This also explains the high selectivity of triacetin when acetic anhydride is used which is contributed to very small amount of molecular water in that situation.

#### 5. Conclusions

The efficient conversion of glycerol to triacetin with acetic anhydride has been successfully performed with magnetic solid acid catalysts. A 100% conversion of glycerol and 99.0% selectivity of triacetin is obtained using the Fe-Sn-Ti (SO<sub>4</sub><sup>2-</sup>)-400 catalyst at 80 °C for 30 min. This exhibits that the magnetic catalytic materials is very promising in the utilization of glycerol. Moreover, there exist the special effects on the reaction temperature and time in the acetylation of glycerol. Furthermore, a possible reaction mechanism is proposed to explain the high conversion and good selectivity of this catalytic process.

#### Acknowledgements

This research work was financially supported by the National Natural Science Foundation of China (21003093) and the State Key Program of the National Natural Science Foundation of China (21336008).

#### References

- [1] H.J. Lee, D. Seung, K.S. Jung, H. Kim, I.N. Filimon, Etherification of glycerol by isobutylene: tuning the product composition, *Appl. Catal. A Gen.* 390 (2010) 235–244.
- [2] F. Frusteri, F. Arena, G. Bonura, C. Cannilla, L. Spadaro, O. Blasi, Catalytic etherification of glycerol by tert-butyl alcohol to produce oxygenated additives for diesel fuel, *Appl. Catal. A Gen.* 367 (2009) 77–83.
- [3] V.L.C. Goncalves, B.P. Pinto, J.C. Silva, C.J.A. Mota, Acetylation of glycerol catalyzed by different solid acids, *Catal. Today* 133 (2008) 673–677.
- [4] P. Ferreira, I.M. Fonseca, A.M. Ramos, J. Vital, J.E. Castanheiro, Acetylation of glycerol over heteropolyacids supported on activated carbon, *Catal. Commun.* 12 (2011) 573–576.
- [5] J. Gui, X. Cong, D. Liu, X. Zhang, Z. Sun, Novel Brønsted acidic ionic liquid as efficient and reusable catalyst system for esterification, *Catal. Commun.* 5 (2004) 473–477.
- [6] D.C. Forbes, K.J. Weaver, Brønsted acidic ionic liquids: the dependence on water of the Fischer esterification of acetic acid and ethanol, *J. Mol. Catal. A Chem.* 214 (2004) 129–132.
- [7] L. Zhou, E. Al-Zaini, A.A. Adesin, Catalytic characteristics and parameters optimization of the glycerol acetylation over solid acid catalysts, *Fuel* 103 (2013) 617–625.
- [8] I. Kim, J. Kim, D. Lee, A comparative study on catalytic properties of solid acid catalysts for glycerol acetylation at low temperatures, *Appl. Catal. B Environ.* 148–149 (2014) 295–303.
- [9] A. Heidekum, M.A. Harmer, Addition of carboxylic acids to cyclic olefins catalyzed by strong acidic ion-exchange resins, *J. Catal.* 181 (1999) 217–222.

- [10] K. Klepacova, D. Mravec, M. Bajus, Brønsted acidic ionic liquids: the dependence on water of the Fischer esterification of acetic acid and ethanol, *Appl. Catal. A Gen.* 294 (2005) 141–147.
- [11] I. Dosuna-Rodríguez, E.M. Gaigneaux, Glycerol acetylation catalysed by ion exchange resins, *Catal. Today* 195 (2012) 14–21.
- [12] P. Lauriol-Garbey, G. Postole, S. Lorida, A. Auoux, V. Belliere-Baca, P. Rey, Acid-base properties of niobium-zirconium mixed oxide catalysts for glycerol dehydration by calorimetric and catalytic investigation, *Appl. Catal. B Environ.* 106 (2011) 94–102.
- [13] P. Ferreira, I.M. Fonseca, A.M. Ramos, J. Vital, Acid -base properties of niobium-zirconium mixed oxide catalysts for glycerol dehydration by calorimetric and catalytic investigation, *Catal. Commun.* 10 (2009) 481–484.
- [14] S.K. Bhorodwaj, D.K. Dutta, Activated clay supported heteropoly acid catalysts for esterification of acetic acid with butanol, *Appl. Clay Sci.* 53 (2011) 347–352.
- [15] P. Ferreira, I.M. Fonseca, A.M. Ramos, J. Vital, J.E. Castanheiro, Glycerol acetylation over dodecatungstophosphoric acid immobilized into a silica matrix as catalyst, *Appl. Catal. B Environ.* 91 (2009) 416–422.
- [16] P. Ferreira, I.M. Fonseca, A.M. Ramos, J. Vital, J.E. Castanheiro, Esterification of glycerol with acetic acid over dodecamolybdophosphoric acid encaged in USY zeolite, *Catal. Commun.* 10 (2009) 481–484.
- [17] J.A. Melero, R. van Grieken, G. Morales, M. Paniagua, Acidic Mesoporous Silica for the Acetylation of Glycerol: Synthesis of Bioadditives to Petrol Fuel, *Energ. Fuel* 21 (2007) 1782–1791.
- [18] I. Kim, J. Kim, D. Lee, Sulfonic acid functionalized deoxycellulose catalysts for glycerol acetylation to fuel additives, *Appl. Catal. A Gen.* 482 (2014) 31–37.
- [19] M.L. Testa, V.L. Parola, L.F. Liotta, A.M. Venezia, Screening of different solid acid catalysts for glycerol acetylation, *J. Mol. Catal. A Chem.* 367 (2013) 69–76.
- [20] M. Huang, X. Han, C. Hung, J. Lin, P. Wu, J. Wu, S. Liu, Heteropolyacid-based ionic liquids as efficient homogeneous catalysts for acetylation of glycerol, *J. Catal.* 320 (2014) 42–51.
- [21] M.S. Khayoon, S. Triwahyono, B.H. Hameed, A.A. Jalil, Improved production of fuel oxygenates via glycerol acetylation with acetic acid, *Chem. Eng. J.* 243 (2014) 473–484.
- [22] S. Kale, S.B. Umbarkar, M.K. Dongare, R. Eckelt, U. Armbruster, A. Martin, Selective formation of triacetin by glycerol acetylation using acidification-exchange resins as catalyst and toluene as an entrainer, *Appl. Catal. A Gen.* 490 (2015) 10–16.
- [23] C. Hammond, S. Conrad, I. Hermans, Simple and scalable preparation of highly active Lewis acidic Sn-beta, *Angew. Chem. Int.* 51 (2012) 11736–11739.
- [24] C. Guo, S. Yao, J. Cao, Z. Qian, Alkylation of isobutane with butenes over solid superacids,  $\text{SO}_4^{2-}/\text{ZrO}_2$  and  $\text{SO}_4^{2-}/\text{TiO}_2$ , *Appl. Catal. A Gen.* 107 (1994) 229–238.
- [25] H. Atia, U. Armbruster, A. Martin, Dehydration of glycerol in gas phase using heteropolyacid catalysts as active compounds, *J. Catal.* 258 (2008) 71–82.
- [26] Y.T. Kim, K.-D. Jung, E.D. Park, Gas-phase dehydration of glycerol over silica-alumina catalysts, *Appl. Catal. B Environ.* 107 (2011) 177–187.